Measuring the Mutual Diffusion Coefficient for Dodecyl Acrylate in Low Molecular Weight Poly(dodecyl acrylate) with Laser Line Deflection (Wiener's Method) and the Fluorescence of Pyrene

Daniel Antrim,[†] Patrick Bunton,[‡] Lydia Lee Lewis,[§] Brian D. Zoltowski,[†] and John A. Pojman*,[†]

Department of Chemistry and Biochemistry, The University of Southern Mississippi, Hattiesburg, Missisippi 39406, Department of Physics, William Jewell College, 500 College Hill, Liberty, Missouri 64068, and Department of Chemistry, Millsaps College, Jackson, Mississippi 39210

Received: January 14, 2005; In Final Form: April 16, 2005

Diffusion of small molecules into glassy polymers is quite complicated and almost always non-Fickian. Little work has been done with the diffusion of low molecular weight polymers that are liquids at room temperature (such as poly(dodecyl acrylate)) into their miscible monomers. We have studied three molecular weights under 20 000 to determine if poly(dodecyl acrylate) diffusion into dodecyl acrylate could be treated with Fick's law and if so to determine the values of the diffusion coefficients. We compare two methods for measuring the diffusion of dodecyl acrylate into poly(dodecyl acrylate): We used laser line deflection (Wiener's method) and improved upon the method from published reports. We also used the dependence of pyrene's fluorescence on the viscosity to measure the concentration distribution, and thus to extract the diffusion coefficient. After an initial relaxation period, diffusion in all cases followed Fick's law with a single concentration-independent diffusion coefficient. Comparison of the diffusion coefficients obtained by both methods yielded the same order of magnitude for the diffusion coefficients (10^{-7} cm^2/s) and showed the same trend in the dependence on the average molecular weight of the polymer (a decrease in the diffusion coefficient with an increase in the molecular weight).

1. Introduction

Korteweg first discussed the possibility that sharp, compositional gradients in miscible fluids could act like interfacial tensions.[1] He proposed that such a transient, or effective, interfacial tension could be represented by a term that accounts for nonlocal interactions, and this term was proportional to the square of the compositional gradient. These interfacial tensions at miscible interfaces have been studied by Zeldovich, who considered the problem of an effective interfacial tension between miscible fluids,[2] and by Joseph and Renardy, who provided a superb review of the topic up to 1992.[3]

We have been investigating the possible role of effective, or transient, interfacial tension in miscible fluids, particularly how such stresses could cause convection at a sharp transition zone between miscible fluids (analogous to Marangoni convection). Specifically, we have shown through simulations that when a Korteweg stress term is added to the Navier−Stokes equations for miscible fluids that convection can indeed occur.[4−6] To accurately perform these simulations, we need to know the nature of the mass transport, or diffusion, between a polymer (e.g., poly(dodecyl acrylate) or PDDA) and its monomer (e.g., dodecyl acrylate or DDA).

There are two general cases of solvent diffusion into polymers:[7] diffusion into a glassy polymer and diffusion into a nonglassy polymer. Solvent diffusion into a glassy polymer is anomalous diffusion (two different diffusion rates for the monomer diffusion into the polymer and the polymer diffusion into the monomer) and cannot be adequately represented by Fick's law or by a single, concentration-independent diffusion coefficient.[7−12] Solvent diffusion into a nonglassy polymer exhibits mutual diffusion, which can be represented by Fick's law and which may be represented by a single, concentration-independent diffusion coefficient.[7] The polymer in our studies of fluid motion induced by Korteweg stresses must be able to flow.[4−6] Thus, low molecular weight PDDA is not a glassy polymer, and these PDDA systems may have mutual diffusion.

We had two goals for this work: To determine if the mutual diffusion of low molecular weight PDDA and DDA could be represented by a single concentration-independent diffusion coefficient and to determine the value of that coefficient for three different molecular weights. We monitored the diffusion of PDDA and DDA by two methods—laser line deflection (LLD or Wiener's method[13]) and the viscosity dependence of ultraviolet-excited fluorescence of pyrene—and determined the diffusion coefficient by three analyses—a Gaussian curve fit (full-curve fit) and the method of Rashidnia et al.[14] for the LLD data and a complementary error-function fit for the fluorescence data.

The two monitoring techniques showed the evolution of an initial, sharp concentration gradient, which experienced a relaxation time of 30 to 50 min after which the system continued to relax according to Fick's law. For the portion of the system that experienced Fickian diffusion, all three analyses provided nearly the same value for the diffusion coefficient for a given molecular weight of the PDDA. The analysis technique of Rashidnia et al.[14] utilized only a portion of the data obtained

* Author to whom correspondence should be addressed. E-mail: john@pojman.com.
[†] The University of Southern Mississippi.
[‡] William Jewell College.
[§] Millsaps College.

10.1021/jp0502609 CCC: $30.25
Published on Web 05/18/2005

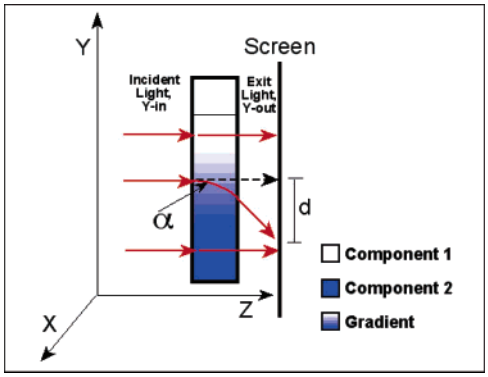

Figure 1. Light deflection of a point laser as it passes through homogeneous and gradient regions. (Reprinted with permission from ref 20.)

by Wiener's method (the profile width), and we improved upon this technique by utilizing all of the concentration data with the Gaussian curve fit. Diffusion coefficients were determined for three molecular weights of PDDA at room temperature showing a decrease in the diffusion coefficient with an increase in molecular weight.

2. Measurement Techniques

2.1a. Laser Line Deflection (Wiener's Method). Diffusive and some reactive systems form concentration gradients between the system's components, and these concentration gradients are manifested as refractive-index gradients. While interferometric techniques are some of the most precise techniques for measuring refractive indices, interferometry is expensive and requires very precise control over the optics as well as protection from vibrations. Jamshidi-Ghaleh et al. have developed a technique that uses Moiré patterns in a less-expensive technique that requires less protection from vibrations and that yields good results.[15] Laser line deflection (LLD), also known as Wiener's method,[13] is an optical technique that is also sensitive to refractive-index gradients, has a lower cost than interferometry, and requires less protection from vibrations. The advantage of LLD over the Moiré technique is the ease of interpretation, although the analysis suffers from the limitation that the gradients must be one-dimensional. LLD has been used to measure diffusion coefficients for butanol and water,[16] glycerol and water,[17,18] and silicone oils of different molecular weights.[14] In addition, Lewis et al. used the method to monitor isothermal frontal polymerization (IFP).[19−21] Similarly to the IFP study, the monomer and polymer in this study are both colorless and form a concentration gradient that is not visible to the naked eye. LLD was used to detect the refractive index gradient. Because the refractive index gradient is proportional to the concentration gradient, Fick's law can be applied to the data to determine the diffusion coefficients. The theory and logistics of LLD relative to these experiments are explained in the following paragraphs.

Normal to the interface plane, light from a laser passes through a sample to focus on a viewing screen behind the sample. When the laser passes through the pure polymer or the pure monomer, the light follows a linear path through the sample, and the light is not deflected because these two components have spatially homogeneous refractive indices (e.g., Component 1 and Component 2 in Figure 1 and the entire sample in Figure 2a). However, at the interface between the diffusing monomer and polymer, a concentration gradient is formed; this concentration gradient causes a refractive-index gradient as illustrated by the "Gradient" regions in Figures 1 and 2b. As the laser light passes through the refractive-index gradient within the sample, the light is deflected at an angle of α, and the light appears on the viewing screen (Figure 1). The larger the refractive index gradient through which the laser light passes, the greater the deflection and the larger the α value.

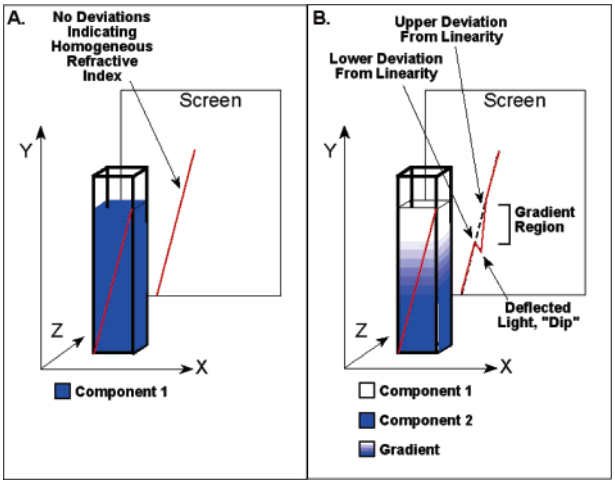

Figure 2. Laser line deflection through a sample of homogeneous refractive index (no light deflection) (A) and through a sample with a refractive-index gradient (deflected light with characteristic "dip") (B). (Reprinted with permission from ref 20.)

If the laser source were a point, either the experimental system or the laser would have to be moved in a vertical direction to view the entire sample. To eliminate this difficulty, a line laser was used to illuminate the entire sample from the upper corner to the opposite lower corner (Figure 2). (The line cannot be vertical, or data from the gradient region will be covered by Component 2's data.) With this line laser, the experimental system yields a characteristic "dip" on the viewing screen (Figure 2b). As indicated in Figure 2b, the area that deviates from the straight line (defined by the upper and lower deviations) is the area where the gradient region exists, and the magnitude of the deviation is proportional to the refractive-index gradient. Figure 3 shows representative LLD images with respect to time of the DDA-PDDA diffusive system and the characteristic dip from the refractive-index gradient.

Initially the gradient region is not symmetrical ($t = 0$ and 60 s) but relaxes with time and becomes symmetrical after 30 to 50 min ($t = 3000$ s). When the monomer is poured onto the polymer, some mixing occurs. (Great care is taken to minimize this mixing.) In addition, the diffusion may not initially be concentration independent, which would result in an asymmetrical dip. This study is interested in the diffusion of the monomer−polymer system that occurs after the 30 to 50 min relaxation time when the dip is symmetrical, and thus when Fick's law can be applied to the system. Thus, all data points in this study used to determine the diffusion coefficients were after the initial relaxation period.

Because the concentration gradient is not linear in the *y*-direction (Figures 1 and 2), the refractive-index gradient is also not linear in the *y*-direction. (The refractive-index gradient continually changes.) Thus, as the light travels through the sample and deflects, the path of deflection has a slight curvature as indicated in Figure 1. Thus, the measured light deflection is an average in the *z*-direction.

2.1b. LLD: Polymer Preparation, Experimental Procedure, and Data Analysis. To run the diffusion experiments with dodecyl acrylate (DDA) and poly(dodecyl acrylate) (PDDA),we prepared three PDDA samples of different molecular

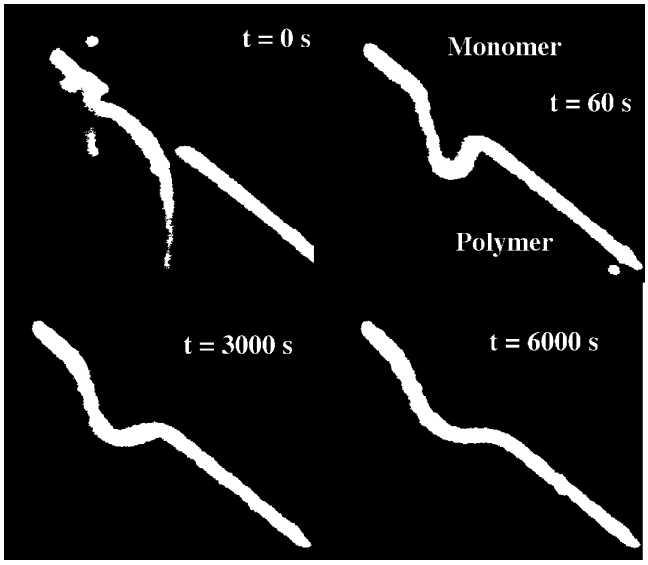

Figure 3. Representative images of the deflected laser line caused by the concentration gradient between the polymer (bottom) and the monomer (top), after four different times. The four times show the progression from asymmetric deflection ($t = 0$ and 60 s) to symmetric deflection (3000 and 6000 s) and are for the lowest molecular weight polymer ($M_w = 1.9 \times 10^4$). The field of view is 1×1 cm.

weights. All samples were prepared with dodecyl acrylate (Sartomer, 90%, $n = 1.440$) as the monomer, Irgacure 184 (Ciba) as a photoinitiator, and dodecyl mercaptan (Sigma Aldrich, 98%) as a chain transfer agent to control the molecular weight. The three samples were made with various concentrations of dodecyl mercaptan in DDA (0.7%, 1.3%, and 2%), 3×10^{-3} M Irgacure, and 10^{-5} M pyrene (Fluka, 99.0%). The samples were irradiated at 365 nm for 90 min with an EFOS Novacure 100-W mercury vapor light source with an intensity of 45 mW cm^{-2}. The molecular weights of the samples were obtained via gel-permeation chromatography (GPC) calibrated with polystyrene standards and with THF as the mobile phase. Representative samples from each of the three molecular weights of the polymers were examined with an Atago Multi-Wavelength Abbe refractometer DR-M2 to determine a refractive index of 1.464, which indicates independence of the refractive index from molecular weight.

To run an LLD diffusion experiment, 2.0 mL of PDDA was poured into a glass cuvette (Starna, $1 \times 1 \times 4$ cm^3) without the polymer touching the sides of the container. DDA (1.0 mL) was layered on top of the PDDA with use of a syringe along the side of the cuvette to minimize mixing. The cuvette was placed into the LLD apparatus within a thermostated blackout box at room temperature (21 ± 2 °C). Images were captured at regular intervals with NIH Image (a frame-capture program) on a Macintosh Quadra. After measuring the pixel width of the cuvette (for pixel to centimeter conversion), the region to be recorded was selected, and the NIH Image software was set for image capturing. After the monomer was injected, the box was closed, and the NIH imaging software was activated. The temperature of the box was obtained after 1 h to ensure that thermal equilibrium had been reached. (For further information on the LLD setup, see ref 20.) Five to eight experiments for each of the three molecular weights were run at the same temperature of 21 ± 2 °C. For each experiment, an image was captured every 10 min for a period of 6 h.

To determine the diffusion coefficients, it was necessary to transform the raw data (images) into data sets proportional to the refractive-index (or concentration) gradient (dn/dy, y)

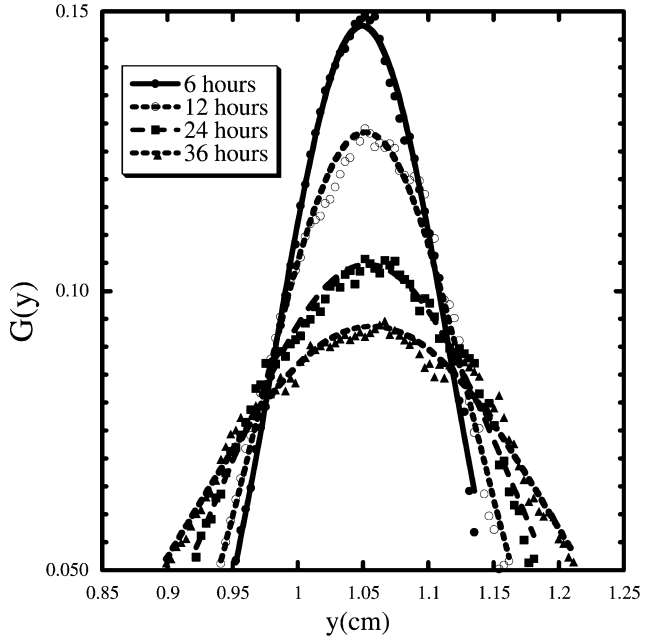

Figure 4. Gradient profiles of LLD experimental data. Gaussian curves (eq 9, full-curve fits) were fit to the profiles. Each set of symbols is the averaged data from a single LLD experiment at a different time during the experiment, and the corresponding lines are the Gaussian fits.

proportional to (y, y'') as explained in the following paragraphs: First the software UN-SCAN-IT was used to assign (x, y) data points to each pixel in a single LLD image. The (x, y) data sets were then imported into a spreadsheet where the data were averaged. Due to the thickness of the laser line, each x value had several y values. To facilitate the data analysis, all y values corresponding to a single x value were averaged.

The characteristic "dip" has an (x, y) coordinate system corresponding to the x- and y-axes of the cuvette (Figure 2b), and the bell-shaped curve has a (y, y'') coordinate system corresponding to the y-axis of the cuvette and to the absolute value of the deflected light distance (referred to in the remainder of the discussion as the "deflected light distance") (eq 1).

$$(y, y'') = (y\text{-axis of the cuvette, } |\text{distance of deflected light}|) \quad (1)$$

The deflected light distance along the y-axis of the cuvette is determined from the absolute value of the difference of the incident light position (y') and of the outgoing light position (y) (eq 2).

$$|\text{deflected light distance in the } y\text{-direction}| = y'' = |y' - y| \quad (2)$$

To determine y' for an individual (x, y) from any frame within an individual sample, a line equation ($y' = mx + b$) for the individual sample is first determined. (The line equation is determined by fitting the data corresponding to the monomer portion of the first frame within said sample to $y' = mx + b$.) The x value of an individual (x, y) is inserted into this line equation to yield y'.

$$\text{position of incident light} = y' = mx + b \quad (3)$$

To determine the diffusion coefficients, a gradient profile (a plot of (y, y'') or the deflected light distance with respect to position along the y-axis of the cuvette) is needed. Figure 4 shows several profiles for different times within a single

experiment, and the y'' values of these profiles are proportional to the refractive-index and concentration gradients (eq 4).

$$y''(y) \propto \frac{dn}{dy} \propto \frac{dC}{dy} \tag{4}$$

In eq 4, n is the refractive index of the monomer, y is the height of the cuvette, and C is the monomer concentration.

We extracted the diffusion coefficients from the gradient profiles using two methods: a curve fit of a Gaussian function (referred to in the remainder of the paper as the "full-curve fit") and the method of Rashidnia et al.,[14] which used the widths of the gradient profiles at two different standardized heights. For both techniques, we assumed the diffusion for the full-curve fit could be treated as diffusion from an infinite region of polymer into an infinite region of monomer: The diffusion model of monomer and a nonglassy polymer assumes that at $t = 0$ the normalized concentration of the monomer goes from 0 in the polymer to 1 in the monomer (no diffusion).[7] Physically, this condition cannot be obtained due to instantaneous mixing of the monomer and polymer during pouring. Thus, this study's goal is to examine the diffusion after the initial relaxation time of the monomer and polymer (approximately 30 to 50 min, or 2000 to 3000 s) where the behavior of the gradient profile went from asymmetrical to symmetrical. In addition, both techniques assumed that the diffusion coefficient was a constant and not a function of concentration. Thus, to derive an expression for the concentration gradient, dC/dy (eq 5), we start with Fick's second law.[7]

$$\frac{dC}{dt} = D\frac{\partial^2 C}{\partial y^2} \tag{5}$$

In eq 5, D is the mutual diffusion coefficient, and t is time within the experiment. (For both analyses, Fick's second law (eq 5) is used. To use this equation, Rashidnia et al. stipulated the following assumptions: the mutual diffusion coefficient and the fluid's density in the area of interest remain constant, and the concentration of the DDA and the PDDA are linearly proportional to their refractive indices.[14]) The solution to this differential equation (eq 6) is a complementary error function (the second term in eq 6).

$$C = \frac{C_0}{2}\left(1 - \frac{2}{\sqrt{\pi}}\int_0^{(x/2)\sqrt{Dt}} e^{-\beta^2}\, d\beta\right) \tag{6}$$

[7] C_0 is the initial monomer concentration. The spatial derivative of eq 6 is a Gaussian function and yields the desired expression for the concentration gradient with respect to distance within the cuvette.[7]

$$\frac{dC}{dy} = A\frac{1}{2\sqrt{\pi Dt}} e^{-y^2/4Dt} \tag{7}$$

A is a constant dependent upon the experimental setup. Because the refractive index (n) is proportional to the polymer concentration, the derivative of the n with respect to position can also be represented by a Gaussian function (eq 8).

$$\frac{dn}{dy} = A\frac{1}{2\sqrt{\pi Dt}} e^{-y^2/4Dt} \tag{8}$$

To determine D for an individual experiment, we fit a Gaussian function (eq 9) to selected gradient profiles over the course of the reaction.[7] The variable m_1 takes into account the

$$G(y) = m_1 e^{-(m_2-y)^2/4m_3} \tag{9}$$

normalization of the data, m_2 provides the center point of the Gaussian, and m_3 is equal to Dt. (Figure 4 shows the fit data for various times within a representative sample.) The diffusion coefficient for the reaction is the slope of the best-fit line of a plot of m_3 (or Dt) versus t (Figure 5). This best-fit line technique assumes that the diffusion coefficients are concentration independent as previously stated, and thus yields an average value for D over the course of a single experiment. To ensure that the diffusion is truly mutual, it is important to ensure that the diffusion "front", the maximum position of the gradient profile, does not move with respect to time. The maximum position of

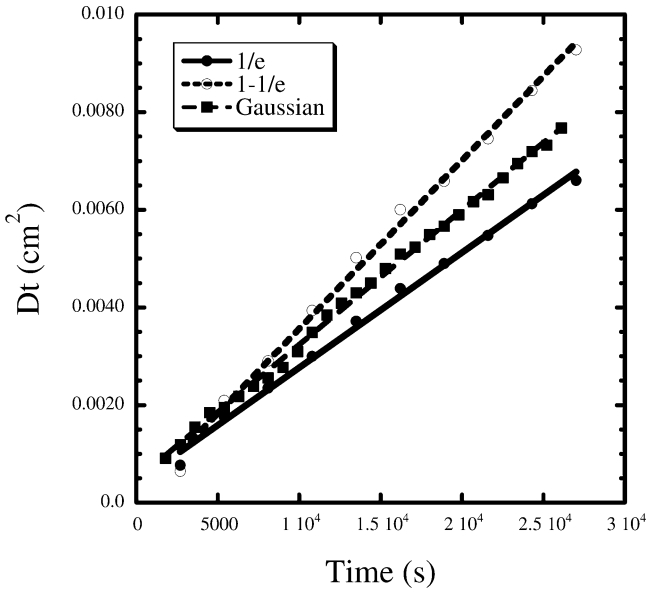

Figure 5. Calculations of the diffusion coefficients for the LLD data, using the full-curve (Gaussian) fit and Rashidnia et al.'s method[14] (plots of 1/e and 1 − 1/e) of fitting the data. Each symbol is the Dt data from a single gradient profile for an individual time during an experiment, and the corresponding lines are the best-line fits.

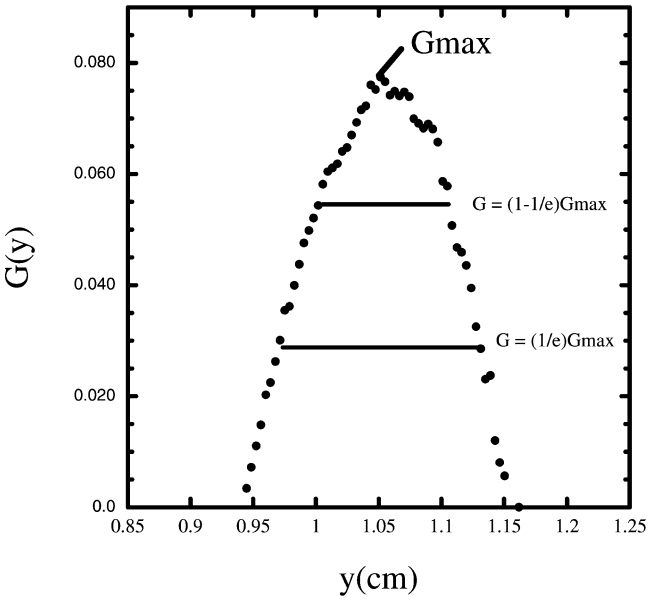

Figure 6. Representative data (gradient profile) illustrating how the different widths were calculated according to Rashidnia et al.'s method.[14]

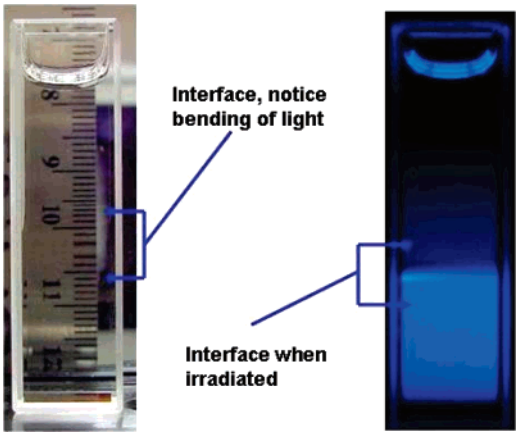

Figure 7. Left: Monomer−polymer interface viewed in normal room light. The interface is indicated by the distortion or lensing of the ruler image. Right: Irradiation of the monomer−polymer system containing 10^{-5} M pyrene. (Fluorescence was not filtered for this image so as to give a clearer image to the eye.) In both images, the monomer is above the polymer. The top of the monomer is denoted by the meniscus. However, the entire sample in the image shown is not illuminated, hence, the dark region. The meniscus is visible due to reflected fluorescence from below. To control the region of illumination, collimated light was passed through a rectangular aperture. (These two images are representative images and do not represent the same interface.)

the gradient profile was determined by visual inspection and did not deviate from its position during the course of the diffusion. To ensure the best Gaussian-curve fit, the center point of the Gaussian was left as a free parameter (m_2) to be determined by the graphing program. The average value and standard deviation were determined for the five to eight experiments of an individual molecular weight. These average values and standard deviations for the three polymer molecular weights are listed in Table 1 in the Results and Discussion section.

The second data-analysis method followed the technique of Rashidnia et al.:[14] Because the gradient profile has the shape of a Gaussian curve, Fick's law (eq 5) could also apply to their technique. They did not use the entire gradient profile to determine D (and, thus, eq 9) but only used the width of the profile at two different standard heights within the curve, $(1/e)G_{max}$ and $(1 - (1/e))G_{max}$ (Figure 6), to yield minimum and maximum values for the diffusion coefficients. (G_{max} is the maximum height of the gradient profile, and $(1/e)G_{max}$ and $(1 - (1/e))G_{max}$ are solutions to the second derivative of Fick's law.) To calculate the value of Dt for an individual gradient profile (and thus, an individual time within the experiment), using Rashidnia et al.'s method, the following procedure was used, and Figure 6 illustrates the relevant parameters: The height of the gradient profile was measured, and the heights at $(1/e)G_{max}$ and $(1 - (1/e))G_{max}$ were calculated. The widths of the gradient profile at these heights were measured and were designated $\delta_{1/e}$ and $\delta_{(1-1/e)}$, respectively. Dt was then calculated for both widths according to the solutions (eqs 10 and 11) of Fick's law for the functions at these two heights.[14]

$$\text{For } (1/e)G_{max}: \qquad Dt_{1/e} = \frac{\delta_{1/e}^{\,2}}{16} \tag{10}$$

$$\text{For } (1 - (1/e))G_{max}: \qquad Dt_{1-(1/e)} = \frac{\delta_{1-(1/e)}^{\,2}}{7.344} \tag{11}$$

Equation 10 yielded a minimum value for Dt, and eq 11 yielded a maximum value for Dt. The values of Dt for various gradient profiles (and thus, various times) within the reaction were

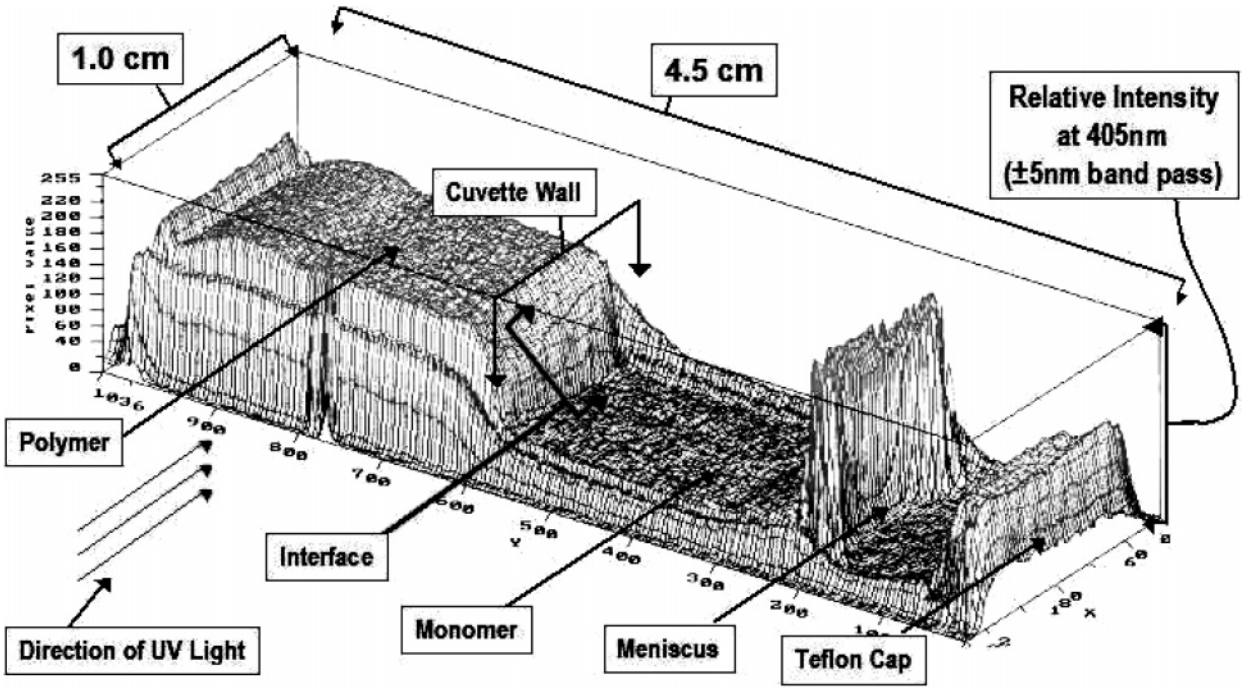

Figure 8. A three-dimensional plot of fluorescence intensity versus the (x, y) position of monomer−polymer sample containing 10^{-5} M pyrene in a cuvette during irradiation at 365 nm. (The left side (labeled 1.0 cm) is the cuvette bottom, the vertical axis is pyrene fluorescence, and the axis perpendicular to the direction labeled "Direction of UV Light" is the cell height. The camera was focused perpendicular to the UV light direction. The filter was 400 nm.) The polymer fluorescence is bright, the monomer fluoresces very little, and the gradient between the monomer and polymer is clearly seen. Proper calibration is then used to convert the fluorescence axes to concentration or viscosity resulting in two-dimensional field information.

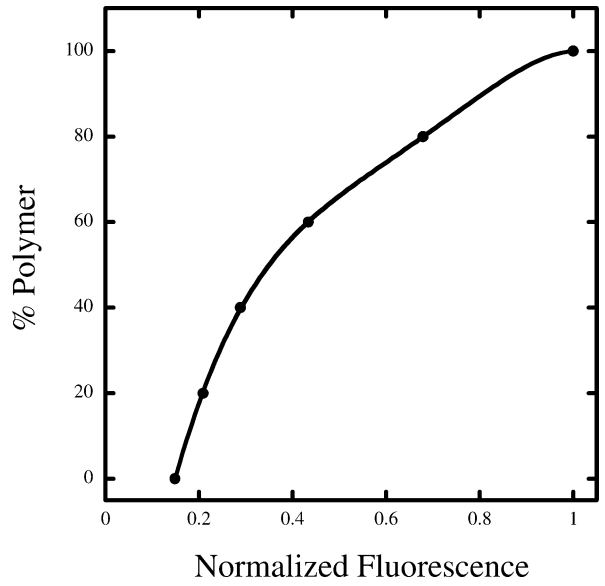

Figure 9. A calibration curve of polymer concentration as a function of the normalized fluorescence at 400 nm. The fluorescence was normalized by dividing by the fluorescence intensity for 100% polymer. The calibration curve is % polymer $= -83.88 + 761x - 1557x^2 + 1557x^3 - 578x^4$, where x is the normalized fluorescence.

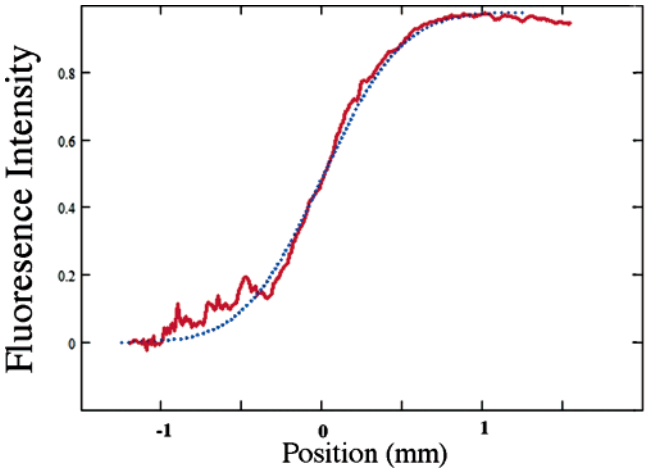

Figure 10. Sample data showing a complementary error function (eq 6) fit to concentration data computed from fluorescence as a function of position across the interface. The solid line is the data and the dotted line is the fit using MathCad (MathSoft Engineering and Education, Inc.).

determined. Two values of the reaction's diffusion coefficient were obtained from the slope of the best-fit line of a plot of m_3 (or Dt) versus t (Figure 5), using the Dt values from both heights (or $(1/e)G_{max}$ and $(1 - (1/e))G_{max}$). Again, this best-fit line technique assumes that the diffusion coefficients are concentration independent as previously stated, and thus yields an average value for D over the course of a single experiment. These two values were then averaged, and a standard deviation was determined for the five to eight experiments of an individual molecular weight. These average values and standard deviations for the three polymer molecular weights are listed in Table 1 in the Results and Discussion section.

2.2a. Fluorescence. The fluorescence shift of small molecules added to polymeric systems has been used as a noninvasive means of monitoring reaction conversion.[22−27] For example, the viscosities of pyrene and its derivatives increase as polymerization occurs, and Migler et al. have used the fluorescence shift of bis-pyrene to measure temperature profiles during polymer processing.[28] Because of viscosity changes associated with diffusive systems, we supposed that the fluorescence of pyrene could be used to measure the concentration gradient of a polymer into its monomer. We developed a method for determining mutual diffusion coefficients of monomer−polymer systems and gauged the method's accuracy by comparison to the full-curve-fit method and Rashidnia et al.'s method.

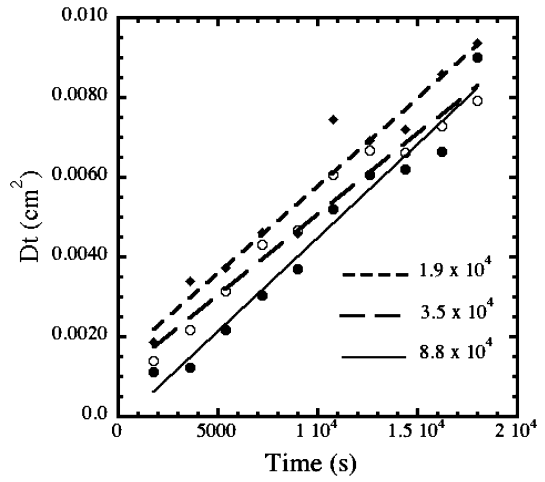

Figure 11. Calculations of the diffusion coefficients from the fluorescence data. Each symbol is the Dt data from a single gradient profile for an individual time during an experiment, each set of data points corresponds to a different molecular weight (as shown by the appropriate legend within the figure) of the polymer, and the corresponding lines are the line fits.

2.2b. Fluorescence: Polymer Preparation, Experimental Procedure, and Data Analysis. The three different molecular weights of PDDA used with the fluorescence experiments were from the same batches used with the LLD experiments. The DDA was also from the same source as the DDA used in the LLD experiments. Polymer (PDDA) and monomer (DDA) were deoxygenated with argon gas prior to formation of the interface, and 10^{-5} M pyrene was added to both the polymer and monomer. An interface was formed between monomer and polymer (both containing pyrene) by layering the DDA on top of the PDDA, using a syringe along the side of the fluorimeter cell (Starna, $1 \times 1 \times 4$ cm^3) to minimize mixing. Light from an EXFO Novacure Mercury light source (365 nm, collimated and filtered) excited the pyrene within the samples. To limit reoxygenation (known to quench fluorescence), an argon gas flow covered the samples at all times. A filter was placed between the sample and camera to filter the light before images were captured. (The filter was either a 400 ± 5 nm band-pass filter or a long-pass filter that allowed the visible light to pass but filtered the ultraviolet light.) To monitor pyrene fluorescence, a digital camera (Sony Mavica MVC-CD1000) captured two-dimensional images of the system. One diffusion sample for each molecular weight of polymer was successfully examined and analyzed. An example image (without filtering) is shown in Figure 7. All diffusion data were taken at room temperature.

After the formation of the interface, images were taken as a function of time. (A representative image is shown in Figure 7 with the horizontal and vertical axes representing the x- and y-axes of the cuvette.) Figure 8 shows a representative image with three dimensions where the z-axis represents the fluorescence intensity. Each three-dimensional image within one experiment was averaged. A subset of x values (near the incident UV side of the cuvette) corresponding to the same y value were averaged to create a single (x, y) coordinate for each y value. This averaging changed the three-dimensional representation of

TABLE 1: Diffusion Coefficients Determined by Three Analyses: Full-Curve Fit, Rashidnia et al.'s Method,[14] and Fluorescence Technique

	diffusion coefficients (cm^2/s)		
	light deflection technique		fluorescence
M_w	full-curve fit (cm^2/s)	method of Rashidnia et al.[14] (cm^2/s)	infinite complementary error function (cm^2/s)
8.8×10^4	3.8×10^{-7} ($\pm 0.8 \times 10^{-7}$)	3.7×10^{-7} ($\pm 0.8 \times 10^{-7}$)	4.1×10^{-7}
3.5×10^4	4.3 X10^{-7} ($\pm 0.3 \times 10^{-7}$)	4.4×10^{-7} ($\pm 0.2 \times 10^{-7}$)	4.4×10^{-7}
1.9×10^4	4.9×10^{-7} ($\pm 2.5 \times 10^{-7}$)	4.0×10^{-7} ($\pm 1.9 \times 10^{-7}$)	4.7×10^{-7}

Figure 8 into a two-dimensional representation with the axes of cuvette height (*y*-axis) and fluorescence intensity.

To convert the fluorescence data to concentration data, previous fluorescence data as a concentration function were used as a calibration: Six samples of known percentages of polymer in monomer were analyzed via the fluorimetry technique to determine the amount of fluorescence exhibited. This amount of fluorescence was normalized, and a graph or calibration curve was produced (Figure 9). (The percentage of polymer in monomer was determined volumetrically for both the polymer and monomer.) After the analysis, the data are concentration as a function of position across the interface. These data were then fit to the infinite complementary error function solution to the diffusion equation (eq 6 and Figure 10). Figure 10 shows a representative curve fit of a concentration profile for a single time within the experiment. (This technique similarly to the light deflection techniques assumed that the diffusion coefficient was a constant and not a function of concentration and that the diffusion after the relaxation period of approximately 30 to 50 min (for which the diffusion coefficients were obtained) yielded a symmetrical profile. In addition, the UV fluorescence emission from pyrene was directly measured at a wavelength of strong emission in PDDA as determined by UV spectroscopy. Since we were working with very small (5 to 10 M) pyrene concentrations, the shift between direct pyrene fluorescence and excimer fluorescence was not measured since the excimer could not be observed at those low concentrations—if it even exists.)

The diffusion coefficient was determined from a complementary error function solution fit to the data every 30 min for 5 h for three samples. The values for *D* were obtained by determining the slope of the best-fit line to plots of the *Dt* values as functions of time (Figure 11 and Table 1).

3. Results and Discussion

Table 1 lists the diffusion coefficients obtained from the two experimental methods (Wiener's (LLD) and fluorescence) and their three analyses for times after the relaxation period of approximately 30 to 50 min (2000 to 3000 s). For Rashidnia et al.'s analysis, the *Dt* data were obtained only at two widths of the gradient profile compared to using the entire gradient profile. It was difficult at times to measure the widths due to a lack of data points at the exact height where the width was being measured—requiring an estimation of the position of the gradient profile at those points. However, the average coefficient values (*D*) obtained were very close to the coefficient values of the full-curve-fit method (within a maximum of 11% for the two higher molecular weights and a maximum of 36% for the lowest molecular weight). The standard deviation introduced by the monitoring and analysis techniques was reported to be ± 0.05 cm for the deflected light position.[20,21] This value translates to approximately 10% of the diffusion coefficient values obtained with Wiener's method. Thus, a difference of 1% above the percent difference introduced by the instrument and analysis techniques for the higher molecular weight samples is a small difference. In fact, the values of *D* calculated by the full-curve-fit method usually fell directly between the minimum and maximum values calculated by Rashidnia et al.'s method. In addition, the Gaussian-curve fits to the data obtained from Wiener's method fit the experimental data quite well justifying the assumptions that the diffusion coefficients were constants and not functions of concentration and that the diffusion coefficients of monomer into polymer and polymer into monomer could be modeled with a single, concentration-independent mutual diffusion coefficient. Thus, both analysis techniques yield good approximations for *D*.

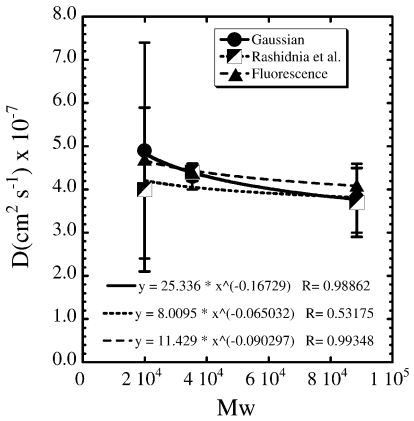

Figure 12. The dependence of the diffusion coefficient on the weight-average molecular weight (M_w). Power functions are fit to all data, and their equations are showed in the figure.

The diffusion coefficients from the fluorescence technique compared well with the coefficients from the light deflection technique (falling within the standard deviation of the diffusion coefficients from the full-curve fit and from Rashidnia et al.'s method). All three methods provide the same order of magnitude for the diffusion coefficients, and the diffusion coefficients calculated from the full-curve fit and the fluorescence data show the same trend in the molecular weight dependence (an increase in diffusion coefficient with a decrease in molecular weight). Thus, the use of pyrene to determine the diffusion coefficients of monomer−polymer systems for low molecular weight polymers is a viable method.

To determine if the diffusion coefficient could be predicted based on the molecular weight of the polymer, the diffusion coefficients for all three methods were plotted with respect to weight-average molecular weight (M_w) (Figure 12). A power function fits well to the results determined with the full-curve fit method and the fluorescence method. In addition, the data determined by the Rashidna et al.'s method agree almost as well.

4. Conclusions

We studied the mutual diffusion of low molecular weight poly(dodecyl acrylate) and dodecyl acrylate using laser line deflection (LLD or Wiener's method) and pyrene fluorescence. The polymers were viscous liquids and, thus, were expected to exhibit Fickian diffusion and have a single, mutual diffusion

coefficient. Both LLD and pyrene fluorescence showed that after an initial time of 30 to 50 min during which the monomer and polymer relax from disruption due to formation of the interface the diffusion process can be modeled with Fick's law by using a concentration-independent diffusion coefficient. We compared the two analysis methods for LLD, and using a full-curve fit to the entire profile obtained results that did not introduce as much experimental error into the procedure. We also demonstrated a novel method for measuring the diffusion coefficient based on the viscosity dependence of the fluorescence of pyrene.

The qualitative trend of increasing diffusion coefficient with a decrease in molecular weight was shown for the diffusion coefficients calculated by the full-curve fit and the fluorescence data. In addition, power functions were fit to the D vs M_w data for all three analysis methods resulting in a possible predictive tool for the diffusion coefficients of monomer−polymer systems having different polymer molecular weights.

Acknowledgment. The authors gratefully acknowledge the work of Mr. Blair Unger (Institute of Optics at Rochester) and Mr. Joseph Huff (Creighton University). Support for this project was provided by NASA's Microgravity Materials Science Program (NAG8-1466 and NAG8-1851) and by the National Science Foundation (CTS -0138660).

References and Notes

(1) Korteweg, D. J. *Arch. Neerl. Sci. Exactes Nat.* **1901**, *6*, 1−24.
(2) Zeldovich, Y. B. *Zh. Fiz. Khim.* **1949**, *23*, 931−935.
(3) Joseph, D. D.; Renardy, Y. Y. *Fundamentals of Two-Fluid Dynamics. Part II. Lubricated Transport, Drops, and Miscible Fluids*; Springer: New York, 1992.
(4) Texier-Picard, R.; Pojman, J. A.; Volpert, V. A. *Chaos* **2000**, *10*, 224−230.
(5) Volpert, V. A.; Pojman, J. A.; Texier-Picard, R. *C. R. Mecanique* **2002**, *330*, 353−358.
(6) Bessonov, N.; Pojman, J. A.; Volpert, V. A. *J. Eng. Math.* **2004**, *49*, 321−338.
(7) Crank, J. *Mathematics of Diffusion*; Clarendon: Oxford, UK, 1975.
(8) Cussler, E. L. *Diffusion*: *Mass Transfer in Fluid Systems*; Cambridge: London, UK, 1997.
(9) Ercken, M.; Adriaensens, P.; Vanderzande, D.; Gelan, J. *Macromolecules* **1995**, *28*, 8541−8547.
(10) Gostoli, C.; Sarti, G. C. *Polym. Eng. Sci.* **1982**, *22*.
(11) Thomas, N. L.; Windle, A. H. *Polymer* **1982**, *23*, 529.
(12) Tihminlioglu, F.; Danner, R. P.; Lutzow, N.; Duda, J. L. *J. Polym. Sci., Part B*: *Polym Phys.* **2000**, *38*, 2429−2435.
(13) Sommerfeld, A. *Optics*: *Lectures of Theoretical Physics*; Academic Press: New York, 1954; Vol. IV.
(14) Rashidnia, N.; Balasubramaniam, R.; Kuang, J.; Petitjeans, P.; Maxworthy, T. *Int. J. Thermophys.* **2001**, *22*, 547−555.
(15) Jamshidi-Ghaleh, K.; Tavassoly, M. T.; Mansour, N. *J. Phys. D*: *Appl. Phys.* **2004**, *37*.
(16) Randall, M.; Longtin, B.; Weber, H. *J. Phys. Chem.* **1941**, *45*, 343−351.
(17) Petitjeans, P.; Maxworthy, T. *J. Fluid Mech.* **1996**, *326*, 37−56.
(18) LaJeunesse, E. Déplacement et Instabilités de Fluides Miscibles et Immiscibles en Cellule de Hele-Shaw. Ph.D. Thesis, Université Paris 6: Paris, France, 1999.
(19) Lewis, L. L.; DeBisschop, C. A.; Volpert, V. A.; Pojman, J. A. In *Nonlinear Dynamics in Polymeric Systems*; ACS Symp. Ser. No. 869; Pojman, J. A., Tran-Con-Miyata, Q., Eds.; American Chemical Society: Washington, DC, 2003.
(20) Lewis, L. L. The Development and Characterizaton of an Optical Monitoring Technique and a Mathematical Algorithm for Isothermal Frontal Polymerization. Ph.D. Thesis, The University of Southern Mississippi: Hattiesburg, MS, 2003.
(21) Lewis, L. L.; DeBisschop, C. A.; Pojman, J. A.; Volpert, V. A. *J. Polym. Sci., Part A.* Accepted for publication.
(22) Valdes-Aguilera, O.; Pathak, C. P.; Neckers, D. C. *Macromolecules* **1990**, *23*, 689−692.
(23) Paczkowski, J.; Neckers, D. C. *Macromolecules* **1992**, *25*, 548−553.
(24) Paczkowski, J.; Neckers, D. C. *J. Polym. Sci., Part A*: *Polym Chem.* **1993**, *31*, 841−846.
(25) Jager, W. F.; Volkers, A. A.; Neckers, D. C. *Macromolecules* **1995**, *28*, 8153−8158.
(26) Okay, O.; Kaya, D.; Pekcan, O. *Polymer* **1999**, *40*, 6179−6187.
(27) Vatanparast, R.; Le, S.; Hakala, K.; Lemmetyinen, H. *Macromolecules* **2000**, *33*, 438−443.
(28) Migler, K. B.; Bur, A. J. *Polym. Eng. Sci.* **1998**, *38*, 213−221.